Jurnal Teknik Indonesia
Volume 5 Nomor 4, November 2026
pp. 1078-1094
DOI: https://doi.org/10.58860/jti.v5i4.944

Evaluation of The Resistance of Deviation Between Levels of Reinforced Concrete Structures Using Zone 3 Design Spectrum in Risk Category II Buildings

Farhan Fadlirahman*, Arief Firmanto
Universitas Swadaya Gunung Jati, Indonesia
Email: farhan.122130143@ugj.ac.id*

Keywords:
Inter-Story Drift; Design Spectrum; SNI 1726:2019; Seismic; P-Delta Risk Category II.

This is an open access article under the CC BY-SA license.

Copyright © 2026 by Author. Published by Publica Scientific Solution

Abstract

This study evaluated the interstory drift performance of the reinforced concrete structure of the Mie Gacoan Central Plant 3 building in Kertajati, Majalengka, Indonesia. Located in an industrial area near the Baribis Fault, the building required a seismic performance assessment to determine its compliance with applicable structural safety requirements. The analysis employed the response spectrum analysis method in accordance with SNI 1726:2019, using ETABS version 22. The results indicated that the structure had a fundamental vibration period of 0.424 seconds in both principal directions, satisfying the prescribed period limitations. The minimum cumulative modal mass participation requirement of 90% was achieved in the eighth mode for the X direction and the seventh mode for the Y direction. Because the initial dynamic base shear was lower than the equivalent static base shear, response spectrum scaling was performed, resulting in scale factors of 1515.27 and 1884.36 in the X and Y directions, respectively. The maximum calculated interstory drift occurred at the second story in the Y direction, reaching 25.014 mm, which remained below the allowable limit of 61.538 mm. Furthermore, the P–Delta stability coefficients for all stories were below 0.10, indicating that second-order effects could be neglected under the applicable stability criteria. These findings demonstrated that the analyzed structure satisfied the evaluated seismic design requirements of SNI 1726:2019 concerning fundamental period, modal mass participation, base shear scaling, interstory drift, and P–Delta stability. However, the results should be interpreted within the scope of the structural model and the seismic performance criteria assessed.

INTRODUCTION

Indonesia is highly susceptible to seismic activity because of its location near the convergence of the Eurasian, Pacific, and Indo-Australian tectonic plates. Interactions among these plates generate substantial tectonic stresses that can trigger earthquakes across various regions of the country (Simanjuntak, 2020). Several provinces, including Aceh, Bengkulu, Banten, West Java, and Central Java, are exposed to significant seismic hazards due to their proximity to active tectonic structures (Damanik et al., 2021; Supendi et al., 2023).

According to a report published by Liputan6.com, citing records from the Indonesian Agency for Meteorology, Climatology, and Geophysics (BMKG), Indonesia experienced 33 damaging earthquakes between January and September 2025. This figure exceeded the annual totals of 5–31 damaging earthquakes reported during 2000–2024. These statistics highlight the

importance of strengthening seismic risk mitigation measures, particularly through structural assessments of buildings located in earthquake-prone regions.

Earthquakes occur suddenly and can cause substantial damage to buildings and infrastructure (Kristianto et al., 2023; Zulfakriza et al., 2024). From a geophysical perspective, tectonic earthquakes result from the sudden release of accumulated strain energy along geological faults, generating seismic waves that propagate through the Earth's crust and produce ground motion (Zebua, 2018). To minimize earthquake-related damage, structural analysis is essential for assessing building performance under seismic loading and identifying potential vulnerabilities that may compromise structural safety (Hilmi et al., 2021; Septiani & Mentari, 2024).

The seismic inertial forces acting on a building are influenced by its mass and ground acceleration, as well as its dynamic characteristics, including stiffness, damping, and natural vibration periods (Akbari et al., 2026). Consequently, seismic-resistant structural design focuses on controlling structural mass, providing adequate lateral stiffness and strength, and ensuring sufficient ductility and energy dissipation capacity. Although earthquake ground motion cannot be controlled, appropriate structural design and detailing can reduce the likelihood of excessive deformation and structural failure.

The Central Plant 3 Mie Gacoan building, located in the Kertajati Industrial Estate, Majalengka Regency, represents an important facility requiring seismic performance assessment. The building serves as a central operational and administrative facility within an industrial area that contributes to regional economic activity. Maintaining its structural integrity is therefore essential not only for ensuring occupant safety but also for supporting operational continuity and minimizing potential economic disruptions following an earthquake.

Majalengka Regency is located within a region influenced by active tectonic structures, including the Baribis Fault system, which contributes to seismic hazards in parts of West Java (Abdalla et al., 2024; Damanik et al., 2021). The Baribis Fault is a significant geological structure extending across portions of northern West Java, with fault segments associated with regional crustal deformation and potential shallow seismic activity (Fakhriati et al., 2024). Earthquakes originating from relatively shallow depths may generate considerable ground shaking near their sources, even when their magnitudes are moderate (Ardha et al., 2025; Hutabarat, 2023; Supendi et al., 2023). Therefore, buildings in the Kertajati industrial area require appropriate seismic design and evaluation based on site-specific seismic hazard parameters rather than geographical proximity to a fault alone.

Considering the building's operational importance and exposure to seismic hazards, its structural performance must be evaluated under earthquake-induced lateral loading in accordance with SNI 1726:2019, Procedures for Earthquake Resistance Design of Building and Nonbuilding Structures. Compliance with applicable seismic design requirements is essential for limiting structural damage, maintaining stability, and protecting building occupants during earthquake events (Setiawan, 2021). Seismic performance assessments should therefore consider both the strength of individual structural components and the overall deformation response of the structural system.

Earthquake-induced structural failures are not determined solely by the magnitude of seismic forces but may also result from inadequate reinforcement detailing, unfavorable structural configurations, and insufficient ductility (Simanjuntak, 2020). In reinforced concrete

structures, inadequate transverse reinforcement confinement in potential plastic hinge regions, insufficient reinforcement development and anchorage lengths, and significant variations in lateral stiffness between stories can contribute to brittle failure mechanisms and excessive deformation. Accordingly, evaluating seismic performance requires consideration of global structural response parameters, particularly interstory drift, which reflects the relative lateral displacement between adjacent floors and provides an important indication of deformation demands on structural and nonstructural components.

Interstory drift is a critical parameter in evaluating the seismic performance of multistory buildings. Excessive interstory drift may damage nonstructural components, increase deformation demands on structural elements, and contribute to instability when second-order P–Delta effects become significant (Cheng et al., 2022; Pujol et al., 2024). Seismic analysis generally involves equivalent lateral force procedures and dynamic analysis methods, including modal response spectrum analysis and response history analysis. Modal response spectrum analysis estimates structural responses using vibration modes and a prescribed design response spectrum, providing an efficient approach for evaluating seismic demands within the limitations specified by applicable design standards. This method was therefore selected to assess the seismic response and interstory drift performance of the reinforced concrete structure examined in this study.

Office buildings generally fall within Risk Category II under SNI 1726:2019 unless their occupancy, function, or other characteristics require a higher classification (Dwirahmanda et al., 2024; Muza'ki & Trimurtiningrum, 2024). Evaluating the seismic performance of such buildings is important because their structural responses depend on local seismic hazard conditions, structural configuration, material properties, and lateral force-resisting systems. Previous studies have examined reinforced concrete building performance using response spectrum analysis in accordance with SNI 1726:2019 (Hilmi et al., 2021; Nasution et al., 2024). For example, research on apartment buildings classified within Earthquake Zone 2 reported interstory drift values within permissible limits, whereas studies examining buildings with different podium configurations in Earthquake Zone 5 identified excessive interstory drift in certain eccentric podium arrangements (Halawa et al., 2025). These findings suggest that structural configuration and seismic loading characteristics can substantially influence interstory drift performance. Nevertheless, further building-specific investigations remain necessary to assess the response of reinforced concrete structures under different seismic design conditions, particularly at the Central Plant 3 Mie Gacoan building in Majalengka, which was examined using the designated Zone 3 design response spectrum.

Based on these considerations, this study aimed to evaluate the interstory drift performance of the reinforced concrete structure of the Central Plant 3 Mie Gacoan building using a special moment-resisting frame system (Sistem Rangka Pemikul Momen Khusus, SRPMK) under the Zone 3 design response spectrum in accordance with SNI 1726:2019. Specifically, the study assessed the fundamental vibration period, cumulative modal mass participation, dynamic base shear requirements, interstory drift limits, and P–Delta stability coefficients to determine compliance with the applicable seismic design criteria. The research was expected to contribute empirical evidence concerning the seismic response of Risk Category II reinforced concrete buildings and provide practical information for structural engineers, building managers, and other stakeholders involved in seismic performance

assessments. Furthermore, the findings were intended to support the evaluation of similar reinforced concrete buildings in industrial areas with comparable structural configurations and seismic hazard characteristics.

METHOD

This study employed a numerical approach using modal response spectrum analysis in accordance with SNI 1726:2019. The analysis was conducted on the Central Plant 3 Mie Gacoan building, located in the Kertajati Industrial Estate, Majalengka Regency, West Java, Indonesia. Structural modeling and dynamic seismic analysis were performed using ETABS version 22 to evaluate interstory drift, lateral displacement, base shear, and cumulative modal mass participation.

The evaluated building was an 8-meter-tall, two-story reinforced concrete structure with a story height of 4 meters. Based on its office function, the building was classified as Risk Category II under SNI 1726:2019. Its lateral force-resisting system was identified as a special reinforced concrete moment-resisting frame (SRPMK), which was considered in the seismic response analysis.

1. Cross-Section Material Data

The specifications of the materials used in this analysis are as follows:

Table 1. Material Specifications

No.	Material	End
1	Concrete	f'c 30Mpa
2	Plain reinforcement steel	BJTP-28
3	Fin reinforcement steel	BJTS-42B

2. Building Column Structure Data

In the CP (*Central Plant*) 3 Mie Gacoan building, the vertical elements use several types of reinforced concrete columns that are adjusted to the position and amount of the load they carry. The details of the dimensions of the modeled columns are presented in Table 2.

Table 2. Column Dimensions

Yes	Column Type	Dimensions
1	Column K1	500x500 mm
2	Column K2	500x500 mm
3	Column K3	400x400 mm

Based on Table 2, the columns of type K1 and K2 have similarities in the cross-sectional size of 500 mm x 500 mm and the diameter of the thread reinforcement used, which is D19. The difference between the two types of columns lies in the number of reinforcements installed, where each type of column shows variations in the number of reinforcements on each floor. More detailed information on this can be seen in Table 3.

Table 3. Column Reinforcement Variations

No	Column Type	Total Reinforcement	
		1st Floor	2nd Floor
1	K1	18 Pieces	12 Pieces
2	K2	14 Pieces	10 Pieces
3	K3	12 Pieces	10 Pieces

3. Building Beam Structure Data

In the CP 3 Mie Gacoan building, the reinforced concrete block type is applied to the horizontal elements of the structure taking into account the position and capacity of the load working on it. The details of the dimensions of the modeled columns are presented in Table 4.

Table 4. Beam Dimensions

No	Beam Type	Dimensions
1	B7	250 x 500 mm
2	B8	250 x 550 mm
3	B9	250 x 600 mm
4	B10	250 x 650 mm
5	B11	300 x 700 mm
6	B12	300 x 750 mm
7	A7	250 x 500 mm
8	C7	250 x 500 mm
9	C8	250 x 550 mm
10	C9	250 x 600 mm
11	C10	250 x 650 mm
12	**C11**	**300 x 700 mm**

From Table 4, there are several types of beam types modeled. Specifically, type B beams function as the main structural element of the load distributor. Type A beams are specifically allocated for cantilever structures. Meanwhile, the type C beam, which is a typical beam, acts as a binding element that distributes the force between the main structural system and the cantilever area.

4. Plate Structure Data

The plates used in the CP 3 Mie Gacoan building are different on the 2nd floor and the roof. The details can be reviewed in Table 5.

Table 5. Floor Plate Data

No.	Plate Type	Thick
1	2nd Floor	130 mm
2	Roof	120 **mm**

5. Load Data

In conducting structural analysis, load definition is a fundamental step to evaluate the behavior of a building against external forces and its natural weight (Halawa et al., 2025). The load analysis on this structure includes three main types of loads, including dead loads, live loads, and earthquake loads.

A. Dead Load

Table 6, Table 7, and Table 8 present the overall dead load values used as a basis in the analysis process.

Table 6. Extra Dead Load Floor Plate

No.	Additional Dead Load Types	Q (kN/m2)
1	Kramik (1 cm)	0.22
2	Stucco (15 cm)	0.36
3	Ceiling Hanger	0.18
4	Electrical Mechanical	0.25
5	Plumbing	0.2
6	Waterproofing	0.03
Total Additional Dead Load		1.24

Based on Table 6, the accumulated additional dead loads acting on the 2nd floor plate reached a value of 0.5056 kN/m². The value of additional dead loads for roof plates is presented in Table 7.

Table 7. Additional Dead Load of Roof Plate

No.	Additional Dead Load Types	Q (kN/m2)
1	Ceiling Frame	0.18
2	Electrical Mechanical	0.25
3	Plumbing	0.2
4	Watreproofing	0.03
Total Additional Dead Load		0.63

Based on Table 7, there is a difference in the value of additional dead loads between the roof plate and the 2nd floor plate, which is 0.32 kN/m² and 0.5056 kN/m², respectively. This condition occurs because the components installed on the roof slab are not as numerous as those on the 2nd floor slab

Table 8. Wall Load

No.	Additional Dead Load Types	Q (kN/m2)
1	Wall load	2.35

The wall is not considered a load-bearing part, so its weight is included as an additional dead load. In modeling, the wall load is modeled in the form of line loads that are channeled towards the connected blocks on the 2nd floor. From table 8, the wall load is modeled at 2.35 kN/m^2.

B. Living Burden

The load caused by the activity and presence of users in a building is categorized as a living load, the values of which are presented in Table 9.

Table 9. Living Burden

No.	Types of Life Load	Q (kN/m2)
1	Indoor Garden	4.79
2	Pantry	4.79
3	Workspace	2.4
4	R. IT Server	2.4
5	R. Leadership Work	2.4
6	Toilet	2.4
7	R. Meeting	2.4
8	Men's Prayer Room	4.7
9	Lounge	4.7
10	Warehouse	6.00
11	R. Projector & Sound	2.4
12	R. Panel	2.4
13	Viewing Area	4.7
14	Multi Purpose Room	4.7

C. Earthquake Load

Spectrum Response Analysis is used in analyzing earthquake loads after SNI 1726: 2019. The object of study is an office building in Kiem Kertajati Industrial Estate. Because the building is included in Risk Category II, the Earthquake Priority Factor (Ie) used is 1.00. From

the available data, the site classification for the location is assumed to be Soft Land (Site Class Se). The value of earthquake acceleration for the bedrock in Kertajati was obtained as Ss = 0.7619 g in a short period and S1 = 0.3527 g in a period of 1 second. The modeling of this structure applies the reinforced concrete Special Moment Bearing Frame System (SRPMK) as the main system in resisting the working seismic forces.

Table 10. Design Spectral Parameters

No	Parameter	Value
1	Ie	1
2	Does	1.3
3	Fv	2.6
4	Sms	0.9905
5	Sm1	0.9170
6	Sds	0.6603
7	Sd1	0.6113
8	T0	0.1852
9	Ts	0.9258
10	TL	20

The calculated spectral response acceleration parameters of the design are the main variables in determining the equivalent earthquake load. These values are then entered into the design spectrum response curve according to the SNI 1726:2019 guidelines, as illustrated in Figure 1.

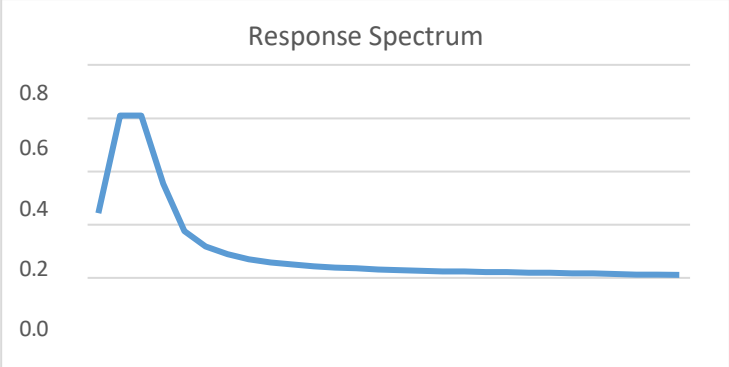


Figure 1. Spectrum Response Graph

Based on the results of the calculation of spectral parameters of the design, the spectral acceleration value of the SDS design was 0.6603 and SD1 was 0.6113. Referring to the limit of SDS values ≥ 0.50 and SD1 ≥ 0.20, this structure is classified as Seismic Design Category D.

RESULTS AND DISCUSSION

1. Fundamental Period of Structure

The fundamental period is one of the most important dynamic parameters in the analysis of the earthquake resistance of a building. This parameter describes the time it takes for the structure to complete one cycle of free vibration after receiving a disturbance. In the analysis of spectrum response according to SNI 1726:2019, the fundamental period has an important role because it directly determines the magnitude or size of the spectral acceleration of the design that will work on the structure. The longer the period of a building, the smaller the

acceleration response, while structures with short periods tend to receive greater earthquake acceleration but have smaller lateral deformations.

The magnitude of the fundamental period is influenced by the mass distribution, rigidity of the structure, height of the building, dimensions of the structural elements, and the lateral force holding system used. According to SNI 1726: 2019, the period used in the calculation must not exceed the maximum period calculated by the formula:

Tmax = With your ×

The calculation of the fundamental period of the approach (Ta) is carried out using the formula

$$Ta = Ct \times hx$$

Where the Ct coefficient is set at 0.0466, and x is 0.9, and the total height of the building is 8 m. As for the value of SD1 = 0.3527 g, the value of the upper limit coefficient of Cu used is 1.4 as stated in Table SNI 1726: 2019

Table 11. Analysis Result Period

Directions	Your	Tmax	Tc	Q,Wear
TX	0,3451	0,483	0,7918	0,483
TY	0,3451	0,483	0,5388	0,483

The results of the analysis showed that the value of the approach period (Ta) was 0.3451 seconds, while the maximum allowable period (Tmax) was 0.424 seconds. Capital analysis using ETABS resulted in a natural period of the structure (Tc) of 0.7918 seconds in the X direction and 0.5388 seconds in the Y direction. The relatively short fundamental period value of this structure also indicates a fairly high level of lateral rigidity even though the building configuration consists of only two floors, so the structure tends to respond to earthquake loads with greater acceleration than multi-storey buildings which generally have a longer vibration period.

The difference in period between the X and Y directions also shows that the distribution of the stiffness of the building in both directions is not entirely identical. A larger period of X direction than Y indicates that the structure has slightly lower rigidity in that direction. This difference is caused by variations in beam configuration, column distribution, and building mass distribution. However, the difference in the period is still within a reasonable range so it does not show any significant structural irregularities

The relatively short period value indicates that the building has a fairly high level of lateral rigidity. The results of this study are also in line with several previous studies on low-rise reinforced concrete buildings which show that structures with regular configurations generally have a relatively short fundamental period due to the dominance of lateral rigidity. Thus, the use of the design period value of 0.424 seconds in this study is considered to be in accordance with the provisions of SNI 1726:2019.

2. Mass Participation

Mass participation is a parameter that measures how much of the total mass distribution of the structure involved or active in each vibrating mode when a building receives an earthquake load. SNI 1726:2019 requires that the number of vibration modes used must be able to produce a minimum mass participation accumulation of 90% in each of the main directions of the building. The requirement aims to ensure that the dynamic response of the entire mass

of the structure has been adequately calculated so that the results of the analysis can be trusted as the basis for evaluating seismic performance.

Table 12. Mass Participation

Mode	SumUX	SumUY
1	0.0376	0.538
2	0.8228	0.5532
3	0.8265	0.8406
4	0.8269	0.8819
5	0.8967	0.8822
6	0.8967	0.8993
7	0.898	0.9901
8	0.9997	0.9916

Based on Table 12, the fulfillment of the requirements for mass participation in a relatively small number of modes (the 7th and 8th modes) means that the structure behaves fairly regularly. The accumulated mass participation of the X direction reached 99.96% in the 8th mode with a period of 0.028 seconds, while the 90% requirement of the Y direction was met one mode earlier, namely in the 7th mode with an accumulation of 98.90%.

The fulfillment of the conditions for mass participation in the relatively early mode also indicates that the distribution of rigidity and mass of the structure in this building behaves fairly regularly, without finding an unnatural dominant vibration mode due to irregularities in shape and mass distribution. In contrast, buildings with irregular shapes usually require a much larger number of modes.

In addition to meeting the requirements of the standard, the high value of mass participation provides confidence that the results of the evaluation of the deviation between levels, internal forces, and basic shear forces obtained from the spectrum response analysis can be used as a basis for decision-making in the evaluation of structural performance. Thus, the results of the variance analysis obtained can be declared valid and representative according to the requirements of SNI 1726:2019, so that it is suitable as a basis for the next stage of structural performance evaluation, including the review of the basic shear force and deviation between levels.

3. Basic Shear Style

In the context of seismic analysis, the base shear force is defined as the peak lateral force acting on the base of the structure due to the influence of earthquakes. Referring to the requirements of SNI 1726:2019, the amount of the minimum dynamic base shear force must be equivalent to the calculated static base shear force. In this study, the Vstatis value was calculated manually using the equivalent lateral force method, while the dynamic V value was obtained directly from the results of the ETAB software analysis. The value of static Vis calculated using the formula:

$$V = Cs \; x \; W$$

Table 13. Basic Shear Styles

Vdasar	Static	Vdynamics	Check
x	982,0826	794,4886	*Scale Up*
y	982,0826	638,9728	*Scale Up*

Based on Table 13, the dynamic basic shear force from the ETABS analysis with an initial scale factor of (SF) = 1,225.83 produces an unscaled dynamic shear force for the direction X = 794.4886kN, and the direction Y = 638.9728kN. A comparison of the static basic shear force of Vstatic = 982.0826kN shows that both dynamic V values are smaller than static V values.

The mismatch between the lower dynamic base shear force of the static base shear force results in the requirement of SNI 1726:2019 not being met, so a scaling process is required for the analysis results. The magnitude of the post-scaling basic shear force is presented in Table 14, while the scale factor applied in the process is listed in Table 15.

Table 14. Basic Shear Force Scaling Results

Directions	Scale Up	Vdynamics	Check
x	1,236	794,4886	OK
y	1,537	638,9728	OK

Table 15. Initial Scale Factor Scaling Results

Directions	Early SF	Scale Up	New SF
x	1225.83	1,236	1515,27
y	1225.83	1,537	1884,36

The calculation of the scale *up factor* for the X direction obtained a magnification ratio value of 1,236 and in the Y direction of 1,537. The value of the magnification ratio obtained is then multiplied by the initial scale factor to produce a new scale factor. Referring to Table 15, a new design scale factor of 1515.2 for the X direction and 1884.36 for the Y direction was obtained.

This new scale factor value is further fed back into the *Load Cases* settings of the response spectrum in the ETABS software to ensure that the entire *internal force output* and deviation of the structure has represented 100% of the planned earthquake force.

The value of the static base shear force V = 982.0826 kN, which is the minimum reference, is obtained from the multiplication between the applicable seismic response coefficient (Cs) and the total effective seismic weight of the structure (W). The initial Cs coefficient is calculated as SDS/(R/Ie) = 0.0825, with the upper limit value Cs,max = SD1/[T×(R/Ie)] = 0.1803 and the lower limit Cs,min = 0.044×SDS×Ie = 0.0291. Because the initial Cs value is between the lower and upper limits, the Cs value = 0.0825 is declared to meet all the requirements of SNI 1726:2019 and is used as Cs to be used in the calculation.

The total effective seismic weight of the structure was obtained from the accumulation of mass on each floor, which was 463,323.85 kg on the roof floor, 589,426.74 kg on the 2nd floor, and 160,546.74 kg on the 1st floor, so that the total mass of the structure reached 1,213,297.33 kg or equivalent to the effective seismic weight W = 11,898 kN.

The difference in the required scale factor between the X direction of 1.236 and the Y direction of 1.537 also indicates that the structure has a lateral stiffness that is not completely uniform in both directions, where the Y direction exhibits a relatively lower dynamic response than the X direction, thus requiring greater scaling to meet the requirements of the minimum base shear force.

4. Deviation Between Levels

Interstory *drift* is one of the main parameters in the evaluation of the seismic performance of multi-storey buildings. This parameter describes the difference in lateral displacement between two adjacent floors due to the influence of earthquake loading. The magnitude of the deviation between the levels reflects the ability of the structure to accommodate deformation without experiencing damage that can interfere with the building's function or reduce the level of safety of its users.

In reinforced concrete structures, the deviation between levels is not only related to the safety of structural elements such as beams and columns, but also greatly affects non-structural elements. Although non-structural elements do not function as the main load bearer, damage to non-structural components can cause significant economic losses and disrupt building operations after an earthquake. Therefore, the evaluation of the deviation between levels is one of the important indicators in assessing the level of suitability of a building against seismic loads.

The lateral displacement difference that occurs between two adjacent floors due to seismic influences is defined as the deviation between levels (story drift) (Çolak et al., 2023). Based on the provisions of article 7.12.1.1 SNI 1726:2019 for Seismic Design Category D, the design deviation at each level (Δ) is not allowed to exceed the value of Δ_a/ρ. By using the redundancy factor ρ = 1.3, the allowable inelastic deviation limit is obtained as follows:

$$\Delta max = D_a/\rho = 0.020hs_x/1.3 = 0.0154hs_x.$$

SNI 1726:2019 stipulates that the calculation of deviation between design levels (Δ) must involve the deflection magnification factor (Cd) as well as the earthquake priority factor (Ie) as stated in the following formula:

$$\Delta = \delta e \times Cd / Ie$$

The initial stage in this evaluation is to review the elastic displacement values at the center of mass of each floor as a result of the software load simulation.

Table 16. Deviation Between Elastic Levels

Story	Displacement		Elastic Drift	
	dX	δy	deX	δeY
3	7.731	8.308	3.225	3.217
2	4.506	5.091	4.060	4.548
1	0.446	0.543	0.446	0.543

Table 16 shows the maximum lateral *displacement* value along with the deviation between the *elastic drift* for X and Y. The displacement value is obtained directly from *the* ETAB analysis output. The deviation between the elastic levels at the level is calculated by looking for the lateral displacement difference between the floor being examined and the floor directly below it.

Table 17. Deviations Between Design Levels

Story	Inelastic Drift	
	ΔX	ΔY
3	17.738	17.694
2	22.330	25.014
1	2.453	2.987

The deviation values between the design levels for the entire floor for both directions are shown in Table 17. With a height between levels of 4000mm, the set clearance deviation value is:

$\Delta a = 0{,}0154 \times 4000$

$\Delta a = 61{,}538$ mm

From the deviation value between the levels and the value of the permit limit, it is then drawn into a graph that can be observed in Figure 2.

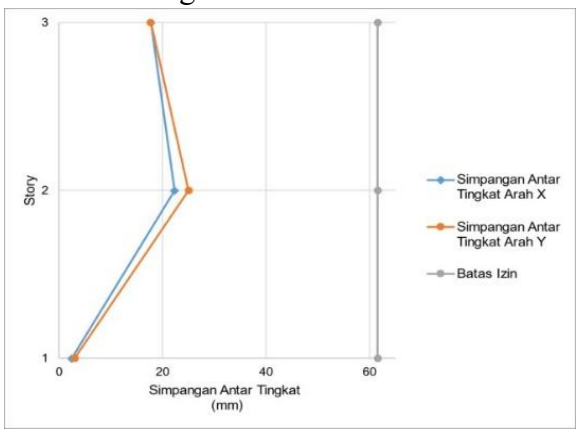


Figure 2. Graph of Deviation Between Levels

The graph above shows that all deviation curves for both directions are far from the permissible limit. The top of the intersection was recorded on the 2nd Floor, which was 25.014 mm in the Y direction.

The results of the analysis showed that the lateral displacement of the structure increased gradually as the elevation of the building increased. In the X direction, the maximum displacement increases from 0.446 mm on the first floor to 4.506 mm on the second floor and reaches 7.731 mm on the roof floor. A similar pattern also occurs in the Y direction, which is from 0.543 mm, increasing to 5.091 mm, then reaching 8.308 mm on the top floor. This pattern is a common characteristic of multi-storey buildings that receive lateral loading, where the top floor experiences the greatest absolute displacement because it is furthest from the point of laying.

When viewed from the lateral displacement pattern, the displacement value of the structure shows a consistent increase from the 1st Floor to the 3rd Floor, namely from 0.446 mm and 0.543 mm on the 1st Floor (X and Y directions), increasing to 4,506 mm and 5,091 mm on the 2nd Floor, to reach the highest values of 7,731 mm and 8,308 mm on the 3rd Floor.

This pattern indicates that the 2nd Floor is the level that receives the most dominant relative lateral force in this structure. In addition, deviations in the Y direction were consistently recorded to be greater than the X direction across the floor, with the most striking difference occurring on the 2nd Floor, in line with the need for a larger Y directional scale factor at the previous stage of basic shear force analysis.

This phenomenon shows that the second floor is the level that experiences the greatest concentration of lateral deformation. There are two-story buildings, most of the inertial forces due to earthquakes are concentrated on the floor above the base of the structure, so the largest relative deviations often appear on the middle or second floors. This condition also shows that the rigidity of the structure between floors is still quite uniform and no indication of the

formation of a soft story or weak story is found, which is a condition when one level has a much lower rigidity than the other.

Overall, the results of the evaluation of the deviation between the levels showed that the Central Plant 3 Mie Gacoan Building had excellent deformation performance. All design deviation values meet the provisions of SNI 1726:2019 with a considerable margin of safety. These results indicate that the structure has sufficient lateral rigidity to control deformation due to the planned earthquake so that the risk of damage to both structural and non-structural elements can be minimized.

5. Effects of P-Delta

The P-Delta effect is the influence of secondary moments that arise due to the combination of the vertical gravitational load (P) on the structure and the lateral deviation (Δ) that occurs due to the working earthquake force (Valdis et al., 2026). In addition to meeting the requirements for intersection between levels, the evaluation of the building's seismic performance must also consider the influence of P-Delta, when the building is deformed due to an earthquake, the gravitational load acting on the column is no longer on the original vertical line so as to produce secondary moments that can magnify the deformation of the structure.

If the influence of P-Delta is large enough, the secondary moment that arises can reduce the effective rigidity of the structure and progressively increase the deviation between levels. In extreme conditions, this phenomenon can cause a loss of structural stability (*instability*) and even trigger an overall collapse. Therefore, evaluation of the P-Delta effect is one of the important requirements in the analysis of earthquake-resistant buildings.

The P-Delta influence control aims to review whether the lateral deformation of buildings that occur due to earthquake loads will give rise to additional secondary moments when combined with gravitational loads. If the value of θ occurs on each floor The result of the calculation of the stability coefficient for both directions, namely the X direction and the Y direction, shows the value of the stability coefficient along with the maximum permissible limit. Details of the results are presented in full in Table 18.

Table 18. Structural Stability Coefficients

Story	Thx	Θ	P - Delta	THMAX
3	0.0075	0.0076	0.1	0.0909
2	0.0151	0.0170	0.1	0.0909
1	0.0019	0.0023	0.1	0.0909

From the evaluations that have been carried out, the entire value of the stability coefficient θ at each level and in each direction does not exceed 0.10 nor the maximum required structural stability coefficient limit.

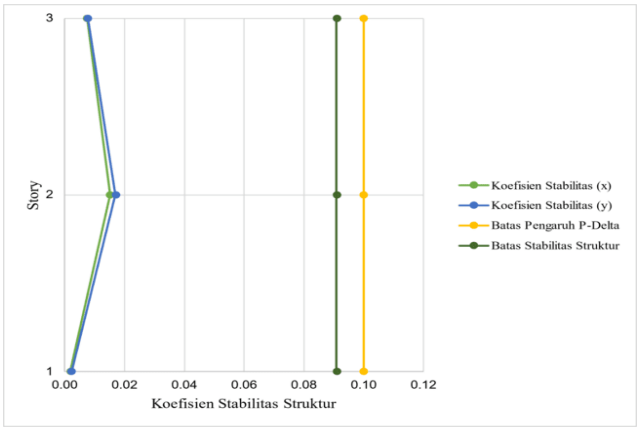


Figure 3. Graph of the Influence of P-Delta

Based on the graph presented, the stability coefficient curve for both directions of the analysis, namely the X direction and the Y direction, shows an almost constricted and uniform distribution pattern. The similarity of the pattern indicates that there is a balance of lateral rigidity of the structure in both directions, so that the structure is able to effectively dampen the influence of secondary moments. Therefore, the effect of P-Delta on the reviewed structure was stated to have no significant impact.

The low value of the P-Delta stability coefficient at all levels of this structure is basically influenced by two main factors. First, the value of the deviation between levels (Δ) is relatively small throughout the floor, especially on the 1st Floor which directly rests on the layout. Second, the magnitude of the seismic shear force (Vx and Vy) on each floor is much more dominant than the cumulative gravitational load (P) at work, so that the ratio between the two remains in a small range.

For comparison, the findings in this study are in line with the results of studies on non-podium buildings and centric podiums in Earthquake Zone 5 which also showed deviations between safe levels, but it was different from the study on eccentric podium types which actually produced deviations that exceeded the permit limit. The comparison further emphasizes that the configuration of vertical and horizontal structures also plays an important role in determining the level of safety of buildings against earthquake forces, in addition to conformity with the quantitative parameters required by SNI 1726:2019.

The results of this study are also consistent with research on low-rise reinforced concrete buildings which show that structures with small inter-level deviations generally produce a stability coefficient well below the permit limit. In contrast, buildings that undergo large lateral deformation or have soft floors tend to show increased P-Delta effects and therefore require further evaluation

In general, the series of analysis results in this study showed consistency between the parameters evaluated, where the relatively short fundamental period, the fulfillment of mass participation in the initial mode, the need for scaling of the basic shear force in both directions, as well as the deviation between levels and the stability coefficient of P-Delta which was far below the permit limit, jointly confirmed that the structure of the Central Plant 3 Mie Gacoan Majalengka Building had lateral rigidity and sufficient deformation capacity to withstand the planned earthquake load in Zone 3 in accordance with the provisions of SNI 1726:2019.

CONCLUSION

Based on the seismic performance assessment of the Central Plant 3 Mie Gacoan building in Majalengka using the designated Zone 3 design response spectrum in accordance with SNI 1726:2019, the analysis indicated that the structure satisfied the evaluated seismic design criteria. The fundamental vibration period was 0.424 seconds in both principal directions. The minimum cumulative modal mass participation requirement of 90% was satisfied in the eighth mode for the X direction (99.97%) and the seventh mode for the Y direction (98.90%). Because the initial dynamic base shear was below the minimum required value, response spectrum scaling was performed, resulting in adjusted scale factors of 1515.27 and 1884.36 in the X and Y directions, respectively. Following this adjustment, the dynamic base shear was equivalent to the required equivalent static base shear of 982.0826 kN. The interstory drift analysis indicated that the calculated drift values at all stories in both principal directions remained within the allowable limits. The maximum interstory drift of 25.014 mm occurred at the second story in the Y direction, remaining below the allowable interstory drift limit (Δa) of 61.538 mm. Furthermore, the calculated P–Delta stability coefficients (θ) remained below the specified threshold of 0.10 and the maximum permissible stability coefficient (θmax) of 0.0909, with the highest calculated value of 0.0170 occurring at the second story in the Y direction. These results indicated that second-order P–Delta effects were not significant under the evaluated loading conditions. Overall, the findings demonstrated that the building satisfied the assessed seismic design requirements of SNI 1726:2019 concerning fundamental period, modal mass participation, base shear scaling, interstory drift, and structural stability. However, these results established compliance only with the evaluated seismic response parameters and did not independently confirm the building's overall earthquake resistance or structural safety.

REFERENCES

Abdalla, H. A., Khalifa, N. D., Lestari, C. A., Mukti, M. M., Gibran, A. K., & Fadlin. (2024). The origin of Baribis Fault and its relationship to the dynamics of Sunda Arc. *Riset Geologi dan Pertambangan*, *34*(1), 55–65. https://doi.org/10.55981/risetgeotam.2024.1311

Akbari, M., Falborski, T., & Jankowski, R. (2026). A novel hybrid seismic control system utilizing the acceleration differential force between a base-isolated Building and an active tuned mass damper inerter under near-field excitations. *Archives of Civil and Mechanical Engineering*, *26*(2), 43.

Ardha, Y. K., Satyarno, I., & Marliyani, G. I. (2025). Probabilistic seismic hazard analysis assessment in Cianjur following the Mw 5.6, 2022 earthquake. *Journal of the Civil Engineering Forum*, *11*(3), 245–256. https://doi.org/10.22146/jcef.18988

Cheng, H., Zhang, R., Zhang, T., Wang, H., Qu, C., & Zhang, P. (2022). P-Delta effects on nonlinear seismic behavior of steel moment-resisting frame structures subjected to near-fault and far-fault ground motions. *Buildings*, *12*(2), 205. https://doi.org/10.3390/buildings12020205

Çolak, H., Türker, H. T., & Coşkun, H. (2023). Accurate estimation of inter-story drift ratio in multistory framed buildings using a novel continuous beam model. *Applied Sciences*, *13*(13), 7819. https://doi.org/10.3390/app13137819

Damanik, R., Supendi, P., Widiyantoro, S., Rawlinson, N., Ardianto, A., Gunawan, E., Husni, Y. M., Zulfakriza, Z., Sahara, D. P., & Shiddiqi, H. A. (2021). Earthquake monitoring of

the Baribis Fault near Jakarta, Indonesia, using borehole seismometers. *Geoscience Letters*, *8*, 38. https://doi.org/10.1186/s40562-021-00209-4

Dwirahmanda, D., Zhafira, T., Winarsih, Y., & Crista, N. H. (2024). Perencanaan pembangunan gedung persewaan kantor 5 lantai Kota Semarang. *Journal of Civil Engineering and Planning*, *5*(2), 238–248. https://doi.org/10.37253/jcep.v5i2.9300

Fakhriati, F., Mu'jizah, M., Supriatin, Y. M., Supriadi, A., Juliastuty, D., Trinirmalaningrum, T., Sururoh, L., Musfeptial, M., Mulyadi, M., & Rusnandar, N. (2024). Local cultural coping strategies to mitigate the impact of Baribis Fault disasters. *Journal of Infrastructure, Policy and Development*, *8*(8), 3551. https://doi.org/10.24294/jipd.v8i8.3551

Halawa, P., Tampubolon, S. P., & Hutabarat, L. E. (2025). Analisis perilaku kinerja struktur bangunan pada variasi tipe podium zona gempa 5 menggunakan metode respon spektrum. *PADURAKSA: Jurnal Teknik Sipil Universitas Warmadewa*, *14*(1), 152–165. https://doi.org/10.22225/pd.14.1.11440.152-165

Hilmi, M., Erizal, & Febrita, J. (2021). Analisis kinerja struktur pada bangunan bertingkat dengan metode analisis respon spektrum berdasarkan SNI 1726:2019. *Jurnal Teknik Sipil dan Lingkungan*, *6*(3), 143–158. https://doi.org/10.29244/jsil.6.3.143-158

Hutabarat, L. E. (2023). Tinjauan geologis gempa Cianjur November 2022. *Jurnal Rekayasa Teknik Sipil dan Lingkungan - CENTECH*, *4*(1), 46–53. https://doi.org/10.33541/cen.v4i1.4836

Kristianto, A., Wiyono, D. R., Setiawan, D., Suhendra, A., & Pranata, Y. A. (2023). Investigasi dan mitigasi struktur bangunan sekolah akibat gempa bumi Cianjur. *Servirisma: Jurnal Pengabdian kepada Masyarakat*, *3*(2), 91–105. https://doi.org/10.21460/servirisma.2023.32.56

Muza'ki, A., & Trimurtiningrum, R. (2024). Analisis kinerja struktur gedung perkantoran pabrik pupuk Gresik dengan pembebanan gempa berdasarkan SNI 1726:2019 terhadap simpangan antar lantai dan pengaruh P-Delta. *JUTIN: Jurnal Teknik Industri Terintegrasi*, *7*(3), 1539–1550. https://doi.org/10.31004/jutin.v7i3.30915

Nasution, I. M., Erizal, & Fauzan, M. (2024). Evaluasi kinerja struktur gedung bertingkat di Jakarta menggunakan pushover analysis. *Jurnal Teknik Sipil dan Lingkungan*, *9*(2), 199–210. https://doi.org/10.29244/jsil.9.2.199-210

Pujol, S., Bedirhanoglu, I., Donmez, C., Dowgala, J. D., Eryilmaz-Yildirim, M., Klaboe, K., Koroglu, F. B., Lequesne, R. D., Ozturk, B., Pledger, L., & Sonmez, E. (2024). Quantitative evaluation of the damage to RC buildings caused by the 2023 southeast Turkey earthquake sequence. *Earthquake Spectra*, *40*(1), 505–530. https://doi.org/10.1177/87552930231211208

Septiani, H., & Mentari, S. (2024). Analisis perilaku gedung Sekolah Dasar Negeri 06 Cijantung terhadap beban gempa menggunakan metode respon spektrum. *Jurnal TESLINK: Teknik Sipil dan Lingkungan*, *6*(1), 194–206. https://doi.org/10.52005/teslink.v6i1.341

Setiawan, D. B. (2021). *Evaluasi kinerja struktur gedung pada kondisi batas layan dan batas ultimit dengan analisis dinamik metode respon spektrum (Studi kasus: Gedung Fakultas Hukum Universitas Sam Ratulangi)* [Tugas akhir, Universitas Islam Indonesia]. DSpace UII. https://dspace.uii.ac.id/handle/123456789/36253

Simanjuntak, P. (2020). Evaluasi kerusakan bangunan akibat gempa di Indonesia. *Jurnal Rekayasa Teknik Sipil dan Lingkungan - CENTECH*, *1*(1), 44–53. https://doi.org/10.33541/cen.v1i1.1425

Supendi, P., Winder, T., Rawlinson, N., Bacon, C. A., Palgunadi, K. H., Simanjuntak, A., Kurniawan, A., Widiyantoro, S., Nugraha, A. D., Shiddiqi, H. A., Ardianto, Daryono, Adi, S. P., Karnawati, D., Priyobudi, Marliyani, G. I., Imran, I., & Jatnika, J. (2023). A

conjugate fault revealed by the destructive Mw 5.6 (November 21, 2022) Cianjur earthquake, West Java, Indonesia. *Journal of Asian Earth Sciences*, *257*, 105830. https://doi.org/10.1016/j.jseaes.2023.105830

Valdis, R., Sapta, S., & Rajela, A. (2026). Analisa pengaruh efek P–Δ terhadap kinerja struktur bangunan bertingkat pada daerah rawan gempa. *Jurnal Multidisiplin Dehasen (MUDE)*, *5*(1), 151–156. https://doi.org/10.37676/mude.v5i1.9531

Zebua, A. W. (2018). Analisis gaya gempa bangunan rumah tinggal di wilayah gempa tinggi. *SIKLUS: Jurnal Teknik Sipil*, *4*(1), 23–35. https://doi.org/10.31849/siklus.v4i1.1128

Zulfakriza, Z., Nugraha, A. D., Heryandoko, N., Ry, R. V., Muttaqy, F., Andika, A., Azhari, M. F., Putra, A. S., Palgunadi, K. H., Cummins, P. R., Supendi, P., Lesmana, A., Sahara, D. P., & Puspito, N. T. (2024). Seismic source analysis of the destructive earthquake November 21, 2022, Mw 5.6 Cianjur (Indonesia) from relocated aftershock. *Scientific Reports*, *14*, 12142. https://doi.org/10.1038/s41598-024-60408-9